International Journal of Innovative Computing, Information and Control
Volume **16**, Number **2**, April **2020**

ICIC International ©2020 ISSN 1349-4198
pp. **571–583**

PRESCRIBED-PERFORMANCE-BASED ADAPTIVE CONTROL FOR HYBRID ENERGY STORAGE SYSTEMS OF BATTERY AND SUPERCAPACITOR IN ELECTRIC VEHICLES

Qian Liu[1], Dezhi Xu[1,*], Bin Jiang[2] and Yongfeng Ren[3]

[1]School of Internet of Things Engineering
Jiangnan University
No. 1800, Lihu Avenue, Wuxi 214122, P. R. China
[*]Corresponding author: xudezhi@jiangnan.edu.cn

[2]College of Automation Engineering
Nanjing University of Aeronautics and Astronautics
No. 29, Yudao Street, Nanjing 211106, P. R. China
binjiang@nuaa.edu.cn

[3]School of Energy and Power Engineering
Inner Mongolia University of Technology
No. 49, Aimin Street, Hohhot 010051, P. R. China
renyongfeng@vip.sina.com

Received September 2019; revised January 2020

Abstract. *To achieve the desired prescribed dynamic and steady-state responses, a prescribed performance control strategy is proposed in electric vehicle system, whose power system is hybrid energy storage system (HESS). The strategy also adopts adaptive control to estimate unknown parameters. Firstly, mathematical models of HESS are derived and the unknown parameters are defined. Secondly, according to the working characteristics of energy storage units (ESUs), battery and supercapacitor are responsible for supplying power to load in different situations. Then, the performance function is considered as a prescribed range for the current tracking error and the corresponding error transformation is introduced. Meanwhile, under the projection operator adaptive law, unknown parameters can be estimated and control laws can be obtained. In addition, the whole system including models and controller is proved to be stable. Finally, simulation results show the effectiveness and superiority of the proposed control strategy.*
Keywords: Battery, Supercapacitor, Projection operator, Adaptive law, Prescribed performance control

1. **Introduction.** With the common development of traditional industry and energy industry, many new problems have arisen such as environmental pollution, energy shortage and low utilization rate of new energy [1, 2]. To improve these conditions, different industries are experimenting and innovating. However, no matter which direction of research and development, the storage and use of energy are the core direction. Because of the limitations of a single ESU, the combination of two or more ESUs with complementary approaches can play a better role in more working environments [3, 4].

Depending on the combination of ESUs, HESS mainly includes the following types: fuel cell-supercapacitor, battery-supercapacitor, fuel cell-battery-supercapacitor, etc. [5, 6, 7]. Fuel cell (FC) offers two main advantages: higher efficiency and zero pollution, but its negative aspects are also apparent. In the process of use, FC cannot recover excess energy and the catalyst requirements are also high. Battery-supercapacitor system is widely

DOI: 10.24507/ijicic.16.02.571

applied on account of technical maturity and wide availability. Because the battery has a relatively low power density per unit cell compared with other energy storage devices, it can be damaged by high peak power or rapid charging/discharging. Supercapacitor (SC) has a high power density, which can provide rapid power fluctuations without a dramatic reduction to protect the battery when large magnitudes and rapid fluctuations in power appear. So in battery-supercapacitor system, battery, serving as the main power source, is efficient at supplying low and steady load power; SC, serving as the auxiliary power source, recovers from rapid power fluctuations [8]. Schematic of the system architecture can be shown in Figure 1, battery and supercapacitor pass through the DC-DC converters separately and then together supply power to the motor.

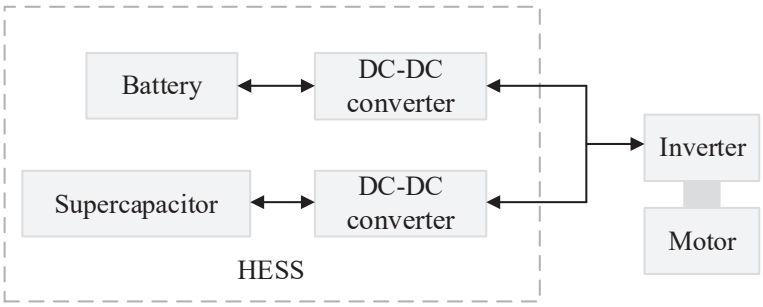

FIGURE 1. Schematic of the system architecture

There are two main research directions of HESS, that is, energy management and control strategy. The idea of energy management is mainly based on the physical property of ESUs, aiming at optimizing allocation. One of the hottest research directions at the moment is the combination with artificial intelligence in order to achieve the goal of low cost and high efficiency [9, 10, 11, 12, 13], but these methods require large amounts of data, so this paper chooses simple distribution methods [14]. Recently, many control strategies of HESS are put forward. In [15, 16], based on sliding-mode control, a Lyapunov-function-based controller is proposed to regulate the DC bus voltage and battery and supercapacitor currents. The sliding mode controller can overcome the uncertainty of HESS and has strong robustness against interference, but it may generate chattering when the state trajectory reaches the sliding mode surface. In [17], a state machine strategy is proposed based on droop control aimed to coordinate multiple power sources and avoid the transients and rapid changes of power demand in a hybrid powertrain configuration. Droop control is the main control strategy for off-grid operation of micro grid. However, according to the current literature, it cannot control the hybrid energy storage system well. In [18], centralized control with high-/low-pass filter is proposed for system net power decomposition and power dispatch. Hierarchical control composed of both centralized and distributed control is proposed to enhance system reliability. However, centralized control has lower reliability and slower speed of response and distributed control has lower system control accuracy. Therefore, high-/low-pass filter is used for power distribution. In [19], a procedure for the design of a near-optimal power management strategy is proposes to improve efficiency and durability. In [20], a control strategy is proposed to smooth the output power of a wind energy system using battery energy storage system, which consists of a fuzzy controller and grid side controller, etc.

However, most references above focus on the study of the steady state performance of the system, ensuring that the tracking error of the system converges to a bounded

region or asymptotically converges to the origin; while the transient performance, that is overshoot and convergence rate, lacks the analysis and design tools of the system. There are many nonlinear control methods for considering steady-state and transient performance, such as [21, 22]. Under the background of the lack of research on improving control performance of existing control methods, Bechlioulis and Rovithakis put forward the concept of prescribed performance, which takes account of both steady and transient performance of the system [23]. Since then, prescribed performance control has been further studied [24, 25, 26]. In [24], a robust dynamic surface controller is proposed with prescribed performance to improve nonlinear feedback systems robustness. In [25], a low-complexity, static and continuous controller is proposed for a class of uncertain, multi-input, multi-output nonlinear systems in order to meet industrial requirements. In [26], the prescribed performance function has been improved to compensate the saturation, mainly changing predetermined performance index to the system convergence time. Based on the mathematical models of the system, HESS is an MIMO nolinear system. So the prescribed performance control can ensure that the tracking error converges to a preset arbitrary small area, the convergence speed and overshoot are guaranteed to meet the preset conditions. There are many methods to estimate unknown parameters, this paper uses adaptive control and projection operator adaptive update laws to achieve dynamic estimation [27, 28].

An HESS with prescribed performance control and adaptive control is proposed in this paper. Based on the energy management strategy, the power of the two parts can be obtained, which can provide reference currents. Because the initial control object is the error between the reference value and the actual value, the prescribed performance control needs to go through error transformation to get the new control object. In practice, the values of resistances, inductances and capacitances are not constant, so they can be expressed as variables, which are estimated by projection operator adaptive update law. The controller can be obtained by Lyapunov function and adaptive update laws. The HESS with prescribed performance control strategy is proved to be stable.

The contributions of the proposed control scheme are summarized as follows. Firstly, the unknown parameters in the system are estimated by adaptive control which adopts adaptive update laws. Besides, prescribed performance control is used to guarantee the transient and steady-state performance. Meanwhile, the controller can be designed by the constraint condition. Finally, as one of nonlinear systems control methods, prescribed performance control can be effectively used in HESS. It is proved that this kind of control can be well used in practical system.

The remainder of this paper is organized as follows. In Section 2, the HESS model is divided into three parts: model of battery operation, model of supercapacitor operation and model of hybrid energy storage system. Each model is described in detail. In Section 3, energy management strategy, prescribed performance control and error transformation are given as control design which contains the idea of adaptive control. The effectiveness of the control strategy is verified by Section 4. In Section 5, some conclusions can be drawn from the controller and simulation results.

2. **The HESS Model.** The topological structure of HESS is illustrated in Figure 2. Battery and supercapacitor are used as ESUs. The working mode of two DC-DC converters is controlled by changing each insulated gate bipolar translator (IGBT) switching duty ratio. SC stands for short of supercapacitor; V_1, V_2, V_3 and V_4 are IGBTs; L_1 and L_2 are inductances, R_1 and R_2 are resistances, C is capacitance; u_B and u_{SC} are the voltage of battery and SC, i_B and i_{SC} are the current of battery and SC, u_O and i_O are output voltage and output current of HESS.

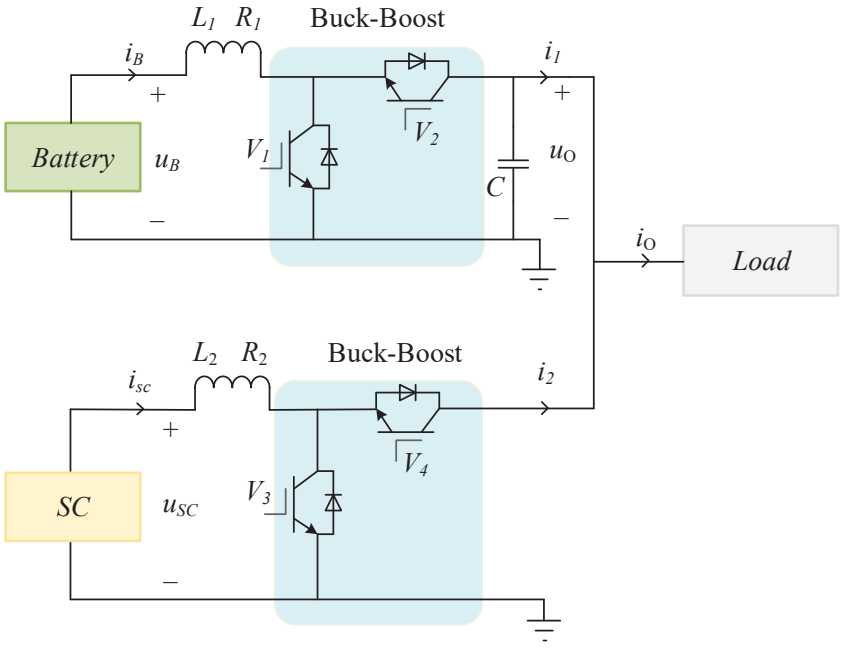

FIGURE 2. Topological structure of the HESS

2.1. **Model of battery operation.** Battery can work in two states, which is controlled by m_{12}. When it is in discharging state, the current direction of i_B is shown in Figure 2 and the switch of IGBT V_1 turns on and V_2 turns off. When it is in charging state, the i_B flows to the battery and the switch of IGBT V_1 breaks and V_2 connects. According to Kirchhoff laws, the charging and discharging state of the battery can be represented by the following model:

$$m_{12} = \begin{cases} 1 - m_1, & i_B^* > 0 \\ m_2, & i_B^* < 0 \end{cases} \tag{1}$$

$$\frac{di_B}{dt} = -\frac{R_1}{L_1} i_B + \frac{1}{L_1} u_B - \frac{m_{12}}{L_1} u_O \tag{2}$$

$$i_1 = m_{12} i_B \tag{3}$$

where R_1 and L_1 are resistance and inductance parameters in a circuit. m_1 and m_2 are the duty cycle of pulse width modulation (PWM) signal. Speaking separately, m_1 represents PWM control signal of IGBT V_1 and m_2 represents PWM control signal of IGBT V_2. m_1 and m_2 have a value of 0 or 1. i_B^* means the current reference of battery. By judging positive or negative value of i_B^*, m_1 and m_2 can be related with m_{12}.

2.2. **Model of supercapacitor operation.** When $i_{SC}^* > 0$, DC/DC converter works in Boost state, supercapacitor discharges; when $i_{SC}^* < 0$, DC/DC converter works in Buck state, supercapacitor charges. The equations of charge/discharge state of supercapacitor can be obtained:

$$m_{34} = \begin{cases} 1 - m_3, & i_{SC}^* > 0 \\ m_4, & i_{SC}^* < 0 \end{cases} \tag{4}$$

$$\frac{di_{SC}}{dt} = -\frac{R_2}{L_2} i_{SC} + \frac{1}{L_2} u_{SC} - \frac{m_{34}}{L_2} u_O \tag{5}$$

$$i_2 = m_{34} i_{SC} \tag{6}$$

where i_{SC}^* means the current reference of supercapacitor and determines the value of m_{34}. m_3 and m_4 represent the continuous duty cycle signal of PWM control input respectively.

2.3. **Model of hybrid energy storage system.** According to the equations above, the mathematical models of HESS can be obtained:

$$\frac{di_B}{dt} = -\frac{R_1}{L_1}i_B + \frac{1}{L_1}u_B - \frac{m_{12}}{L_1}u_O \tag{7}$$

$$\frac{di_{SC}}{dt} = -\frac{R_2}{L_2}i_{SC} + \frac{1}{L_2}u_{SC} - \frac{m_{34}}{L_2}u_O \tag{8}$$

$$\frac{du_O}{dt} = \frac{m_{12}}{C}i_B + \frac{m_{34}}{C}i_{SC} - \frac{1}{C}i_O \tag{9}$$

The parameters R_1, R_2, L_1, L_2 and C are not constant in practice because of the dynamic change. Set these parameters as unknown values and define them as follows:

$$\sigma_1 = \frac{1}{L_1} = \frac{1}{L_2},\ \sigma_2 = \frac{R_1}{L_1} = \frac{R_2}{L_2},\ \sigma_3 = \frac{1}{C} \tag{10}$$

Putting Equation (10) into the models (7), (8) and (9), the HESS models can be converted to

$$\frac{dX_1}{dt} = -\sigma_2 X_1 - m_{12}\sigma_1 X_3 + \sigma_1 u_B \tag{11}$$

$$\frac{dX_2}{dt} = -\sigma_2 X_2 - m_{34}\sigma_1 X_3 + \sigma_1 u_{SC} \tag{12}$$

$$\frac{dX_3}{dt} = m_{12}\sigma_3 X_1 + m_{34}\sigma_3 X_2 - \sigma_3 i_O \tag{13}$$

where X_1, X_2 and X_3 mean i_B, i_{SC} and u_O, respectively. In models (11), (12) and (13), the HESS is a nonlinear system, m_{12} and m_{34} are the controller of HESS, which provide effective PWM waves. And Equation (13) shows u_O is related to i_B, i_{SC}, m_{12}, m_{34} and σ_3, so the control method needs to be selected according to the situation.

3. Control Design.

3.1. **Energy management strategy.** This part mainly arranges the power situation of each ESU according to the physical characteristics. Battery is one kind of energy storage medium and has higher energy density and lower power density. Unlike battery, supercapacitor is power storage media, which is low energy density and high power density. When in stable working state, battery plays a leading role, but in high rate of charge and discharge, supercapacitor provides peak power.

The power relationship between ESUs and load is gained below:

$$P_{Bref} + P_{SCref} = P_{Load} \tag{14}$$

where P_{Load} is the load required power, P_{Bref} is battery reference power, and P_{SCref} is the reference power of supercapacitor. P_{Bref} and P_{SCref} are simply distributed through a filter. Meanwhile, the current reference values i_B^* and i_{SC}^* are written as

$$\begin{aligned} i_B^* &= \frac{P_{Bref}}{u_B} \\ i_{SC}^* &= \frac{P_{SCref}}{u_{SC}} \end{aligned} \tag{15}$$

3.2. **Prescribed performance control and error transformation.** Taking i_B, i_{SC} and u_O as control objects, the tracking error variables e_1, e_2 and e_3 are defined as

$$e_1 = X_1 - i_B^* \tag{16}$$

$$e_2 = X_2 - i_{SC}^* \tag{17}$$

$$e_3 = X_3 - u_O^* \tag{18}$$

where the meaning of u_O^* is different from i_B^* and i_{SC}^*. u_O is the HESS model output voltage and u_O^* can affect the size of u_O. In $P_{Load} = u_O i_O$, if P_{Load} and u_O are determined values, i_O is certain. $i_B + i_{SC} = i_O$, so i_B and i_{SC} are coupled to each other. e_1 and e_2 can be controlled by prescribed performance control, and e_3 can be controlled by virtual controller.

According to [26], performance functions can be used as the performance bounds to constrain the control objects and achieve the desired control objectives. The accepted concepts are as follows.

Definition 3.1. *A smooth function $\rho(t) : R^+ \to R^+$ will be called a performance function if: 1) $\rho(t)$ is positive and decreasing; 2) $\lim_{t\to\infty} \rho(t) = \rho_\infty > 0$.*

Under the requirement of Definition 3.1, $\rho(t)$ is commonly expressed as

$$\rho(t) = (\rho_0 - \rho_\infty)e^{-kt} + \rho_\infty \tag{19}$$

where ρ_0, ρ_∞ are positive constants and $\rho_0 > \rho_\infty$. As the decreasing rate of exponential form, k is positive constants and provides the minimum convergence speed.

Tracking errors are constrained by performance functions, which can meet the following conditions:

$$\begin{cases} -\delta_i\rho_i(t) < e_i(t) < \rho_i(t), & \text{if } e_i(0) \geq 0 \\ -\rho_i(t) < e_i(t) < \delta_i\rho_i(t), & \text{if } e_i(0) < 0 \end{cases} \tag{20}$$

where $0 \leq \delta_i \leq 1$. According to the value of $e_i(0)$, the constraint condition of $e_i(t)$ is divided into two cases. Equation (20) cannot be used directly in the controller, so error transformation system is needed to change constrained problem into an equivalent unconstrained one. The error transformation function is defined as

$$e_i(t) = \rho_i(t)L_i(\varepsilon_i) \tag{21}$$

where $e_i(t)$ is tracking error, $\rho_i(t)$ is performance function, ε_i is the transformed error, and $L_i(\varepsilon_i)$ is a function of the transformed error, which is a smooth, strictly increasing and invertible function. And the function $L_i(\varepsilon_i)$ is defined as follows:

$$\begin{cases} -\delta_i < L_i(\varepsilon_i) < 1, & \text{if } e_i(0) \geq 0 \\ -1 < L_i(\varepsilon_i) < \delta_i, & \text{if } e_i(0) < 0 \end{cases} \tag{22}$$

where the transformed error $\varepsilon_i \in (-\infty, +\infty)$. If $e_i(0) \geq 0$, $\lim_{\varepsilon\to-\infty} L_i(\varepsilon_i) = -\delta_i$, $\lim_{\varepsilon\to+\infty} L_i(\varepsilon_i) = 1$. Otherwise, $\lim_{\varepsilon\to-\infty} L_i(\varepsilon_i) = -1$, $\lim_{\varepsilon\to+\infty} L_i(\varepsilon_i) = \delta_i$.

According to the above conditions, the function $L_i(\varepsilon_i)$ can be obtained:

$$L_i(\varepsilon_i) = \begin{cases} \dfrac{e^{\varepsilon_i} - \delta_i e^{-\varepsilon_i}}{e^{\varepsilon_i} + e^{-\varepsilon_i}}, & \text{if } e_i(0) \geq 0 \\ \dfrac{\delta_i e^{\varepsilon_i} - e^{-\varepsilon_i}}{e^{\varepsilon_i} + e^{-\varepsilon_i}}, & \text{if } e_i(0) < 0 \end{cases} \tag{23}$$

From Equations (21) and (23), ε_i can be rewritten as

$$\varepsilon_i = L_i^{-1}\left(\frac{e_i(t)}{\rho_i(t)}\right) = \begin{cases} \frac{1}{2}\ln\frac{z_i+\delta_i}{1-z_i}, & \text{if } e_i(0) \geq 0 \\ \frac{1}{2}\ln\frac{z_i+1}{\delta_i-z_i}, & \text{if } e_i(0) < 0 \end{cases} \tag{24}$$

where $z_i = \frac{e_i(t)}{\rho_i(t)}$. The derivative of ε_i is

$$\dot{\varepsilon}_i = \frac{\partial L_i^{-1}}{\partial\left(e_i/\rho_i\right)}\frac{1}{\rho_i}\left(\dot{e}_i - \frac{\dot{\rho}_i e_i}{\rho_i}\right) = h_i\left(\dot{e}_i - v_i\right) \tag{25}$$

where $h_i = \frac{\partial L^{-1}}{\partial(e_i/\rho_i)}\frac{1}{\rho_i}$, $v_i = \frac{\dot{\rho}_i e_i}{\rho_i}$.

3.3. **System stability analysis.** Defining the adaptive estimation error:

$$\tilde{\sigma}_i = \hat{\sigma}_i - \sigma_i, \quad i = 1, 2, 3 \tag{26}$$

where σ_i and $\hat{\sigma}_i$ mean actual and reference values of adaptive estimation, respectively.

The prescribed performance control is mainly used to limit the errors, so e_1 and e_2 are replaced by the corresponding transformed error. For errors and unknown parameters, the Lyapunov function can be constructed as

$$V = \frac{1}{2h_1}{\varepsilon_1}^2 + \frac{1}{2h_2}{\varepsilon_2}^2 + \frac{1}{2}{e_3}^2 + \frac{1}{2r_1}\tilde{\sigma}_1^2 + \frac{1}{2r_2}\tilde{\sigma}_2^2 + \frac{1}{2r_3}\tilde{\sigma}_3^2 \tag{27}$$

Taking the known equations into the derivative of Equation (27) with respect to time, the derivative equation is simplified into

$$\begin{aligned} \dot{V} &= \varepsilon_1(\dot{e}_1 - v_1) + \varepsilon_2(\dot{e}_2 - v_2) + e_3\dot{e}_3 + \frac{\tilde{\sigma}_1\dot{\tilde{\sigma}}_1}{r_1} + \frac{\tilde{\sigma}_2\dot{\tilde{\sigma}}_2}{r_2} + \frac{\tilde{\sigma}_3\dot{\tilde{\sigma}}_3}{r_3} \\ &= \varepsilon_1\left(-\hat{\sigma}_2 X_1 - m_{12}\hat{\sigma}_1 X_3 + \hat{\sigma}_1 u_B - \dot{i}_B^* - v_1\right) \\ &\quad + \varepsilon_2\left(-\hat{\sigma}_2 X_2 - m_{34}\hat{\sigma}_1 X_3 + \hat{\sigma}_1 u_{SC} - \dot{i}_{SC}^* - v_2\right) \\ &\quad + e_3\left(m_{12}\hat{\sigma}_3 X_1 + m_{34}\hat{\sigma}_3 X_2 - \hat{\sigma}_3 i_O - \dot{u}_O^*\right) \\ &\quad + \tilde{\sigma}_1\left(\frac{1}{r_1}\dot{\hat{\sigma}}_1 + \varepsilon_1\left(m_{12}X_3 - u_B\right) + \varepsilon_2\left(m_{34}X_3 - u_{SC}\right)\right) \\ &\quad + \tilde{\sigma}_2\left(\frac{1}{r_2}\dot{\hat{\sigma}}_2 + \varepsilon_1 X_1 + \varepsilon_2 X_2\right) \\ &\quad + \tilde{\sigma}_3\left(\frac{1}{r_3}\dot{\hat{\sigma}}_3 + e_3\left(-m_{12}X_1 - m_{34}X_2 + i_O\right)\right) \end{aligned} \tag{28}$$

where $\dot{\tilde{\sigma}}_i = \dot{\hat{\sigma}}_i - \dot{\sigma}_i$, $i = 1, 2, 3$, σ_i is slowly time-varying, so the value of $\dot{\sigma}_i$ can be ignored.

Considering $\dot{V} \geq 0$, the adaptive update laws are designed in order to satisfy the stability requirements:

$$\dot{\hat{\sigma}}_1 = r_1 proj(\hat{\sigma}_1, -\varepsilon_1(m_{12}X_3 - u_B) - \varepsilon_2(m_{34}X_3 - u_{SC})) \tag{29}$$

$$\dot{\hat{\sigma}}_2 = r_2 proj(\hat{\sigma}_2, -\varepsilon_1 X_1 - \varepsilon_2 X_2) \tag{30}$$

$$\dot{\hat{\sigma}}_3 = r_3 proj(\hat{\sigma}_3, e_3(m_{12}X_1 + m_{34}X_2 - i_O)) \tag{31}$$

where function $proj(\cdot)$ represents the projection operator, its role is to constrain parameter estimates and its conclusion is divided into continuous and discrete cases [27, 28]. In this

paper, HESS is a continuous system, so the conclusions of projection operator are as follows:

$$\begin{aligned} &\text{Property 1} \qquad \hat{\psi} \in \Omega_{\psi} \triangleq \left\{ \hat{\psi} : \psi_{\min} \leq \hat{\psi} \leq \psi_{\max} \right\} \\ &\text{Property 2} \qquad \tilde{\psi} \left[proj \left(\hat{\psi}, \tau \right) - \tau \right] \leq 0, \quad \forall \tau \end{aligned} \tag{32}$$

In order to meet Lyapunov stability theory, the first half of Equation (28) can be defined as

$$-n_1 \text{sgn}\varepsilon_1 = -\hat{\sigma}_2 X_1 - m_{12}\hat{\sigma}_1 X_3 + \hat{\sigma}_1 u_B - \dot{i}_B^* - v_1 \tag{33}$$

$$-n_2 \text{sgn}\varepsilon_2 = -\hat{\sigma}_2 X_2 - m_{34}\hat{\sigma}_1 X_3 + \hat{\sigma}_1 u_{SC} - \dot{i}_{SC}^* - v_2 \tag{34}$$

$$-n_3 \text{sgn}e_3 = (m_{12} X_1 + m_{34} X_2 - i_O)\hat{\sigma}_3 - \dot{u}_O^* \tag{35}$$

where $n_1 > 0$, $n_2 > 0$ and $n_3 > 0$. And $\text{sgn}(\cdot)$ is expressed as

$$\text{sgn}(x) = \begin{cases} x/|x| & x \neq 0 \\ 0 & x = 0 \end{cases} \tag{36}$$

where by the transformation of Equations (33), (34) and (35), the following conclusions can be obtained:

$$m_{12} = \frac{1}{\hat{\sigma}_1 X_3} \left(n_1 \text{sgn}\varepsilon_1 - \hat{\sigma}_2 X_1 + \hat{\sigma}_1 u_B - \dot{i}_B^* - v_1 \right) \tag{37}$$

$$m_{34} = \frac{1}{\hat{\sigma}_1 X_3} \left(n_2 \text{sgn}\varepsilon_2 - \hat{\sigma}_2 X_2 + \hat{\sigma}_1 u_{SC} - \dot{i}_{SC}^* - v_2 \right) \tag{38}$$

$$\dot{u}_O^* = \left(m_{12} X_1 + m_{34} X_2 - i_O \right) \hat{\sigma}_3 + n_3 \text{sgn}e_3 \tag{39}$$

Combining the above equations, $\dot{V}$ can be limited to the following:

$$\dot{V} \leq -n_1 |\varepsilon_1| - n_2 |\varepsilon_2| - n_3 |e_3| \leq 0 \tag{40}$$

This implies that the transformation errors ε_1, ε_2 and tracking error e_3 are asymptotically stable with the implement of the proposed controller.

Remark 3.1. *According to Equation (40), the transformation errors ε_1, ε_2 and tracking error e_3 are asymptotically stable, which guarantees ε_i will converge to 0. If the parameter δ_i is selected as 0, ε_i will reach infinity. So based on Equation (24), the time response of e_1 and e_2 are uniformly ultimately bounded.*

4. **Simulink Results and Analysis.** In this section, the HESS with the proposed prescribed performance control strategy is built in MATLAB/Simulink software environment to demonstrate the effectiveness of the proposed control strategy. The structure of the whole system including the relationship between modules and variables is shown in Figure 3. From HESS, u_B and u_{SC} can be measured in HESS model and are the input of energy management strategy model. i_B and i_{SC} are the output parameters of HESS and represent the actual currents. i_B^* and i_{SC}^* are the output parameters of energy management strategy model and represent the reference currents. The errors between actual and reference currents are defined. Prescribed performance model determines the prescribed performance functions according to the errors. Adaptive observer model passes the definitions of system's unknown parameters to the controller. The controller model collects the parameters and outputs m_{12} and m_{34} to HESS. The numerical values used in the simulation are written in Table 1.

The corresponding conclusions can be obtained from the simulation results. The load power distribution can be shown in Figure 4, which generally has two scenarios. When P_{Load} is positive and has no high-frequency power, this means that system is powering

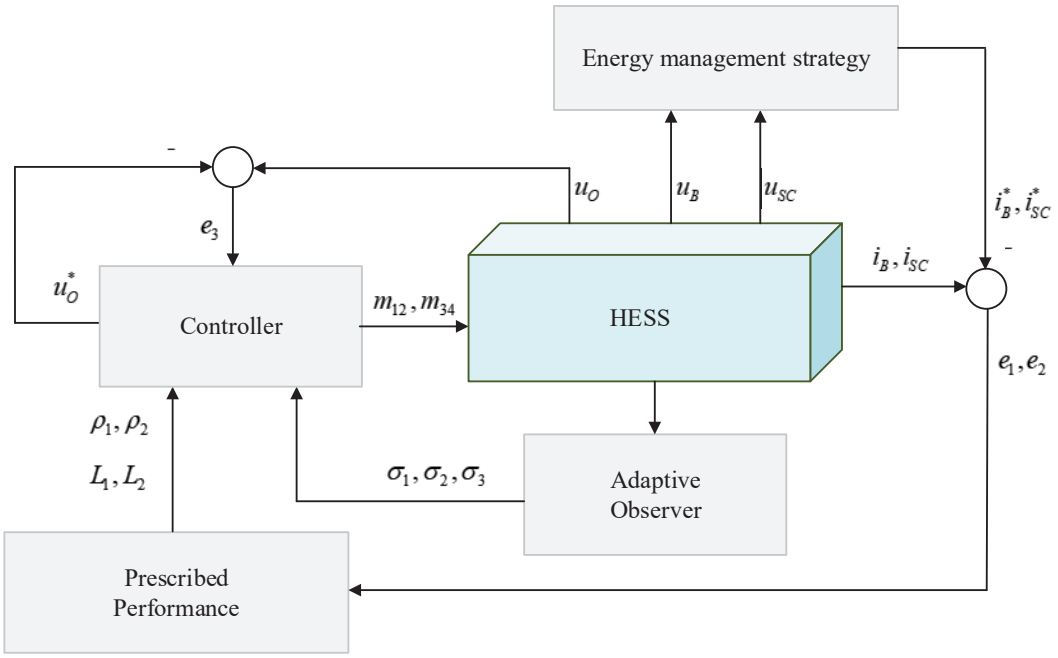

FIGURE 3. The structure of the prescribed performance control and adaptive control for the HESS

TABLE 1. The parameters of HESS and the proposed control scheme

Factors	Parameters	Value
Model parameters	battery	200Vdc, 100Ah, Li-Ion
	supercapacitor	200Vdc, 2000F
	L_1, L_2	3.3mH
	R_1, R_2	20mΩ
	C	16mF
Gains of controllers	n_1	18000
	n_2	18000
	n_3	10000
Gains of prescribed performance	k_1, k_2	1.5, 3
	ρ_{10}, ρ_{20}	50, 10
	$\rho_{1\infty}$, $\rho_{2\infty}$	4, 1
	δ_1, δ_2	0.5, 0.5
Gains of adaptive law	r_1, r_2, r_3	0.2, 0.2, 0.2

the load; when its parameter is negative, it indicates that the system is in the state of absorbing power or automobile braking condition. Whatever the case, battery and SC are responsible for providing different power according to their physical properties. The actual power distribution is shown in Figure 5. In the starting time, the initial values of prescribed performance are large, so the power varies a lot. When it runs for a while, P_B and P_{SC} are consistent with Figure 4. The curve of P_B changes obviously and the curve of P_{SC} has no obvious changes, but they both meet the set power distribution requirements.

From Figures 6 and 7, the tracking curves of i_B and i_{SC} can be respectively compared. At the initial time, the tracking effect is poor due to the initial value of prescribed performance. However, after a while, the current i_B varies up and down i_B^*, which means

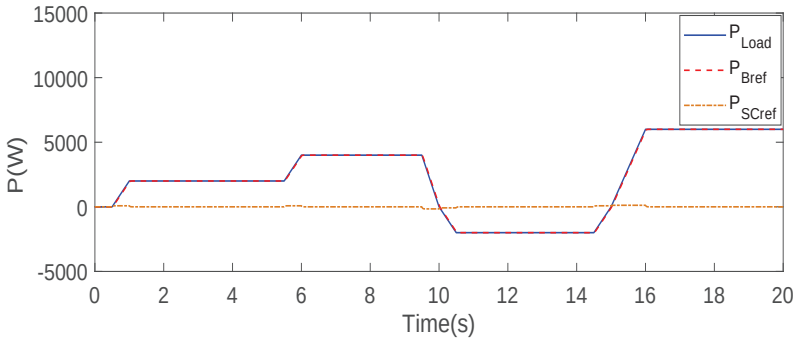

FIGURE 4. The load power distribution profile

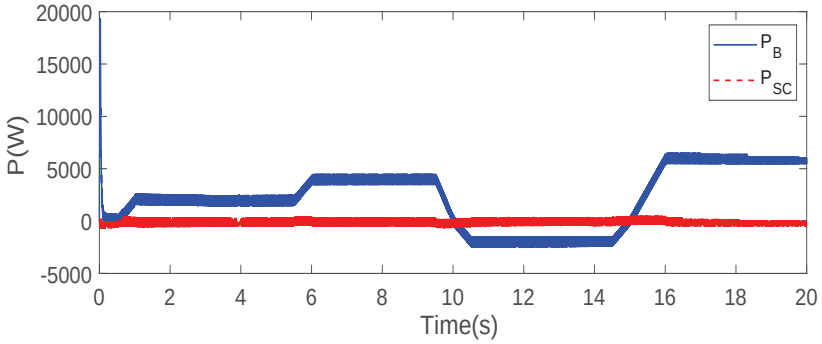

FIGURE 5. The power responses of battery and SC

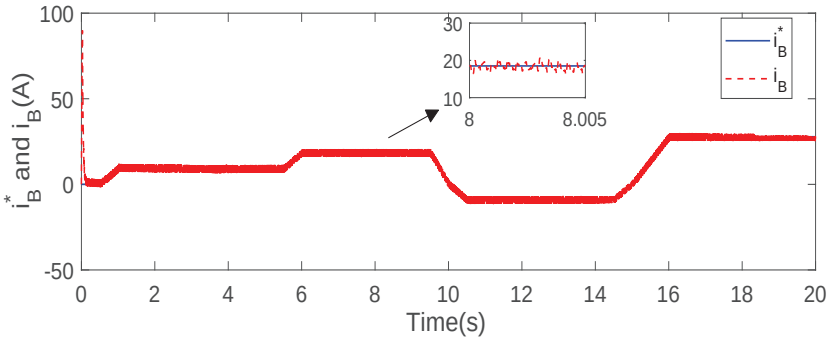

FIGURE 6. The tracking diagram of reference battery current

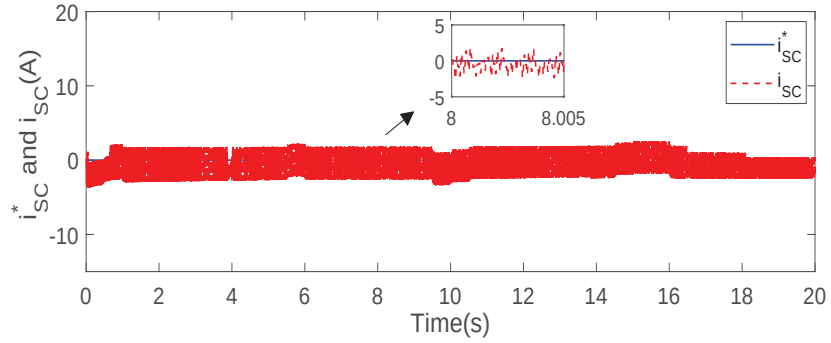

FIGURE 7. The tracking diagram of reference SC current

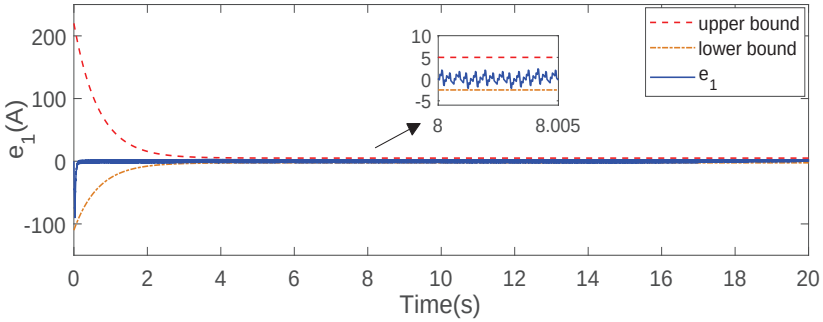

FIGURE 8. The current tracking error of battery

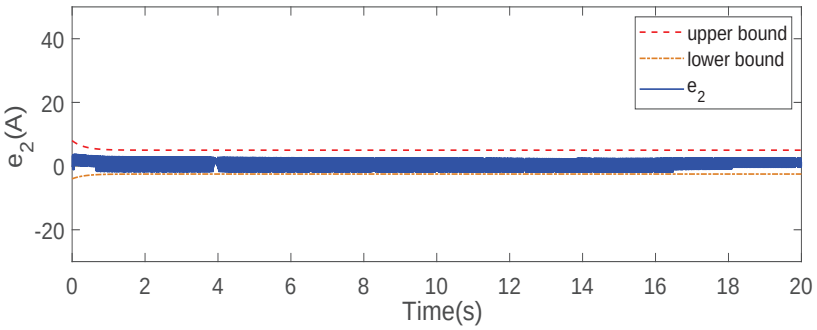

FIGURE 9. The current tracking error of SC

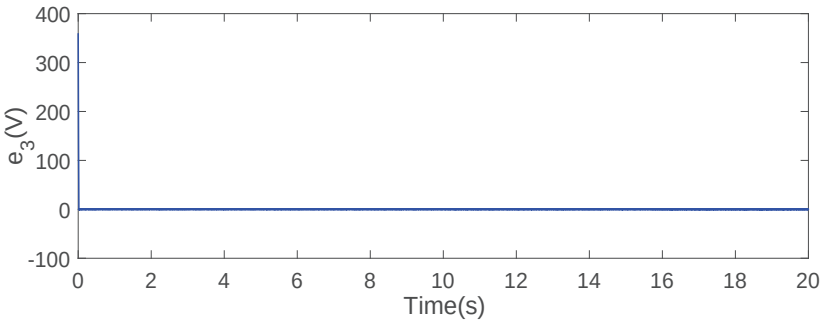

FIGURE 10. The voltage tracking error of u_O

the current i_B can follow up i_B^*. In Figure 7, i_{SC} also tracks i_{SC}^* well. The timeliness and accuracy of current tracking indicate that the control performance of the system is good. In Figures 8-10, e_1, e_2 and e_3 are respectively shown. The tracking errors e_1 and e_2 drawn in Figures 8 and 9 further reveal the favorable tracking performance with tiny error. e_1 and e_2 are located in the prescribed range which means that the defined prescribed performance functions play a good control role. In addition, the voltage tracking error e_3 is large at the beginning of operation but is almost zero after stabilization in Figure 10. Therefore, e_3 is in line with the expected control effect.

In Figure 11, u_O is around 400 volts, which means HESS can output a relatively stable voltage in the case of load power variation. This makes practical sense for the electric vehicle.

5. **Conclusions.** In this paper, a hybrid energy storage system with prescribed performance control is proposed. The control strategy contains energy management strategy,

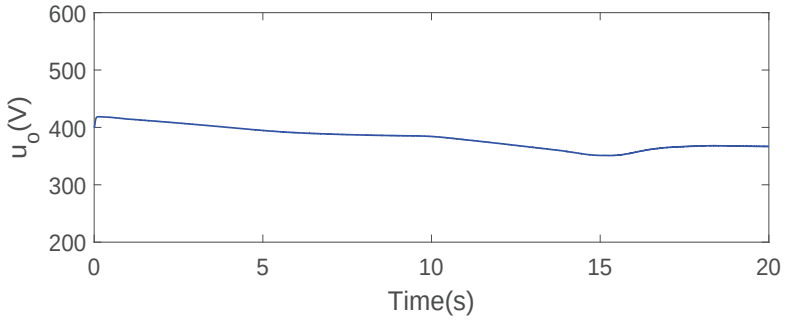

FIGURE 11. The tracking effect on DC link voltage u_O

prescribed performance control and error transformation. First, the uncertain parameters in the system are represented by a projection operator and estimated by an adaptive law. Second, the transient and steady-state performance of parameters is guaranteed by prescribed performance control. Then, the control strategy ensures that the each tracking error converges to a predetermined arbitrary small area and the convergence speed and overshoot meet the predetermined conditions. In the following work, the working environment and performance characteristics of battery and supercapacitor will be investigated. On this basis, efficient and timely energy management strategy will be researched.

Acknowledgment. This work is partially supported by National Natural Science Foundation of China (61973140, 51967016, 51567020), National First-Class Discipline Program of Food Science and Technology (JUFSTR20180205), Fundamental Research Funds for the Central Universities (JUSRP41911), Inner Mongolia Autonomous Region Science and Technology Plan Funding Project (201802035), Natural Science Foundation of Inner Mongolia of China (2015MS0532), Inner Mongolia Electric Power Group (Co., Ltd.) Technology Project (201906).

The authors also gratefully acknowledge the helpful comments and suggestions of the reviewers, which have improved the presentation.

REFERENCES

[1] M. R. Anuar and A. Z. Abdullah, Challenges in biodiesel industry with regards to feedstock, environmental, social and sustainability issues: A critical review, *Renewable and Sustainable Energy Reviews*, vol.58, pp.208-223, 2016.

[2] R. Gerlagh, N. A. Mathys and T. O. Michielsen, Energy abundance, trade and specialization, *The Energy Journal*, vol.36, no.3, pp.235-245, 2015.

[3] A. Zhuk, K. Denschikov, V. Fortov, A. Sheindlin and W. Wilczynski, Hybrid energy storage system based on supercapacitors and li-ion batteries, *Journal of Applied Electrochemistry*, vol.44, no.4, pp.543-550, 2014.

[4] L. Kouchachvili, W. Yaïci and E. Entchev, Hybrid battery/supercapacitor energy storage system for the electric vehicles, *Journal of Power Sources*, vol.374, pp.237-248, 2018.

[5] H. El Fadil, F. Giri, J. M. Guerrero and A. Tahri, Modeling and nonlinear control of a fuel cell/supercapacitor hybrid energy storage system for electric vehicles, *IEEE Transactions on Vehicular Technology*, vol.63, no.7, pp.3011-3018, 2014.

[6] A. Castaings, W. Lhomme, R. Trigui and A. Bouscayrol, Comparison of energy management strategies of a battery/supercapacitors system for electric vehicle under real-time constraints, *Applied Energy*, vol.163, pp.190-200, 2016.

[7] H. Armghan, I. Ahmad, N. Ali, M. F. Munir, S. Khan and A. Armghan, Nonlinear controller analysis of fuel cell-battery-ultracapacitor-based hybrid energy storage systems in electric vehicles, *Arabian Journal for Science and Engineering*, vol.43, no.6, pp.3123-3133, 2018.

[8] T. Ma, H. Yang and L. Lu, Development of hybrid battery-supercapacitor energy storage for remote area renewable energy systems, *Applied Energy*, vol.153, pp.56-62, 2015.
[9] M. G. Carignano, R. Costa-Castelló, V. Roda, N. M. Nigro, S. Junco and D. Feroldi, Energy management strategy for fuel cell-supercapacitor hybrid vehicles based on prediction of energy demand, *Journal of Power Sources*, vol.360, pp.419-433, 2017.
[10] B. Wang, J. Xu, B. Cao and X. Zhou, A novel multimode hybrid energy storage system and its energy management strategy for electric vehicles, *Journal of Power Sources*, vol.281, pp.432-443, 2015.
[11] M. E. Choi, J. S. Lee and S. W. Seo, Real-time optimization for power management systems of a battery/supercapacitor hybrid energy storage system in electric vehicles, *IEEE Transactions on Vehicular Technology*, vol.63, no.8, pp.3600-3611, 2014.
[12] P. Singh and P. Dwivedi, Integration of new evolutionary approach with artificial neural network for solving short term load forecast problem, *Applied Energy*, vol.217, pp.537-549, 2018.
[13] M. Wieczorek and M. Lewandowski, A mathematical representation of an energy management strategy for hybrid energy storage system in electric vehicle and real time optimization using a genetic algorithm, *Applied Energy*, vol.192, pp.222-233, 2017.
[14] I. Azizi and H. Radjeai, A new strategy for battery and supercapacitor energy management for an urban electric vehicle, *Electrical Engineering*, vol.100, no.2, pp.667-676, 2018.
[15] Z. Song, J. Hou, H. Hofmann, J. Li and M. Ouyang, Sliding-mode and Lyapunov function-based control for battery/supercapacitor hybrid energy storage system used in electric vehicles, *Energy*, vol.122, pp.601-612, 2017.
[16] D. Xu, Q. Liu, W. Yan and W. Yang, Adaptive terminal sliding mode control for hybrid energy storage systems of fuel cell, battery and supercapacitor, *IEEE Access*, vol.7, pp.29295-29303, 2019.
[17] Q. Li, H. Yang, Y. Han, M. Li and W. Chen, A state machine strategy based on droop control for an energy management system of pemfc-battery-supercapacitor hybrid tramway, *International Journal of Hydrogen Energy*, vol.41, no.6, pp.16148-16159, 2016.
[18] J. Xiao, P. Wang and L. Setyawan, Hierarchical control of hybrid energy storage system in DC microgrids, *IEEE Transactions on Industrial Electronics*, vol.62, no.8, pp.4915-4924, 2015.
[19] S. Zhang, R. Xiong and J. Cao, Battery durability and longevity based power management for plug-in hybrid electric vehicle with hybrid energy storage system, *Applied Energy*, vol.179, pp.316-328, 2016.
[20] R. I. Putri, F. Ronilaya and M. Rifa'i, A sensorless power smoothing method for a grid-connected wind energy system based on fuzzy interference system, *ICIC Express Letters*, vol.12, no.9, pp.887-895, 2018.
[21] Z. Li, X. Zhang, C. Y. Su and T. Chai, Nonlinear control of systems preceded by preisach hysteresis description: A prescribed adaptive control approach, *IEEE Transactions on Control Systems Technology*, vol.24, no.2, pp.451-460, 2015.
[22] J. Back and H. Shim, Adding robustness to nominal output-feedback controllers for uncertain nonlinear systems: A nonlinear version of disturbance observer, *Automatica*, vol.44, no.10, pp.2528-2537, 2008.
[23] C. P. Bechlioulis and G. A. Rovithakis, Prescribed performance adaptive control of SISO feedback linearizable systems with disturbances, *The 16th Mediterranean Conference on Control and Automation*, IEEE, pp.1035-1040, 2008.
[24] H. Song, T. Zhang, G. Zhang and C. Lu, Robust dynamic surface control of nonlinear systems with prescribed performance, *Nonlinear Dynamics*, vol.76, no.1, pp.599-608, 2014.
[25] A. Theodorakopoulos and G. A. Rovithakis, Low-complexity prescribed performance control of uncertain MIMO feedback linearizable systems, *IEEE Transactions on Automatic Control*, vol.61, no.7, pp.1946-1952, 2015.
[26] C. Zhang, G. Ma, Y. Sun and C. Li, Observer-based prescribed performance attitude control for flexible spacecraft with actuator saturation, *ISA Transactions*, vol.89, pp.84-95, 2019.
[27] Y. Wu, Y. Li, J. Li and S. Zhang, Adaptive resource allocation and capacity comparison of OFDMA and MC-CDMA schemes based on imperfect power-line CSI, *International Journal of Innovative Computing, Information and Control*, vol.14, no.2, pp.437-454, 2018.
[28] H. Wang, B. Chen, C. Lin, Y. Sun and F. Wang, Adaptive neural control for MIMO nonlinear systems with unknown dead zone based on observers, *International Journal of Innovative Computing, Information and Control*, vol.14, no.4, pp.1339-1349, 2018.